

Order from Disorder in Graphene Quantum Hall Ferromagnet

Dmitry A. Abanin, Patrick A. Lee, Leonid S. Levitov

Department of Physics, Massachusetts Institute of Technology, 77 Massachusetts Ave, Cambridge, MA 02139

Valley-polarized quantum Hall states in graphene are described by a Heisenberg O(3) ferromagnet model, with the ordering type controlled by the strength and sign of valley anisotropy. A mechanism resulting from electron coupling to strain-induced gauge field, giving leading contribution to the anisotropy, is described in terms of an effective random magnetic field aligned with the ferromagnet z axis. We argue that such random field stabilizes the XY ferromagnet state, which is a coherent equal-weight mixture of the K and K' valley states. The implications such as the Berezinskii-Kosterlitz-Thouless ordering transition and topological defects with half-integer charge are discussed.

Gate-controlled graphene monolayer sheets[1] host an interesting two-dimensional electron system. Recent studies of transport have uncovered, in particular, anomalous Quantum Hall effect [2, 3], resulting from Dirac fermion-like behavior of quasiparticles. Most recently, when magnetic field was increased above about 20 T, the Landau levels (LL) were found to split [4], with the $n = \pm 1$ and $n = 0$ levels forming two and four sublevels, respectively, as illustrated in Fig.1a. The observed splittings were attributed to spin and valley degeneracy lifted by the Zeeman and exchange interactions.

The physics of the interaction-induced gapped quantum Hall state is best understood by analogy with the well-studied quantum Hall bilayers realized in double quantum well systems [5]. In the latter, the interaction is nearly degenerate with respect to rotations of pseudospin describing the two wells. As a result, the states with odd filling factors are characterized by pseudospin O(3) ordering, the so-called quantum Hall ferromagnet (QHFM) [5]. The pseudospin z component describes density imbalance between the wells, while the x and y components describe the inter-well coherence of electron states. Several different phases [6, 7] are possible in QHFM depending on the strength of the anisotropic part of Coulomb interaction, controlled by well separation.

In the case of graphene, with all electrons moving in a single plane, the valleys K and K' play the role of the two wells in the pseudospin representation with the lattice constant replacing the inter-well separation. To assess the possibility of QHFM ordering, we note that the magnetic length at the 10–30 T field is much greater than the lattice constant. Thus graphene QHFM can be associated with the double-well systems with nearly perfect pseudospin symmetry of Coulomb interaction [8, 9, 10]. Our estimate, presented below, yields anisotropy magnitude of about 10 μK at $B \sim 30$ T, which is very small compared to other energy scales in the system.

Can some other mechanism break pseudospin symmetry more efficiently? Coupling to disorder seems an unlikely candidate at first glance. However, there is an interesting effect that received relatively little attention, which is strain-induced random gauge field introduced by Iordanskii and Koshelev [11]. To clarify its origin, let

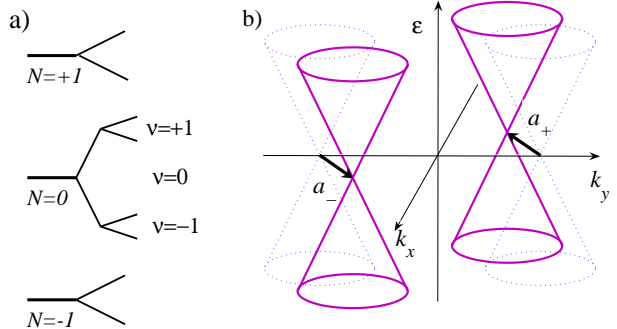


FIG. 1: a) Graphene Landau level splitting, Ref.[4], attributed to spin and valley polarization. When the Zeeman energy exceeds valley anisotropy, all $N = 0$ states are spin-polarized, with the $v = \pm 1$ states valley-polarized and the $v = 0$ state valley-unpolarized. b) The effect of uniform strain on electron spectrum, Ref.[11], described by Dirac cones shift in opposite directions from the points K and K' . Position-dependent strain is described as a random gauge field, Eq.(2).

us consider the tight-binding model with spatially varying hopping amplitudes. Physically, such variation can be due to local strain, curvature [12, 13] or chemical disorder. With hopping amplitudes t_i for three bond orientations varying independently, we write

$$\begin{bmatrix} 0 & \tau(\mathbf{q}) \\ \tau^*(\mathbf{q}) & 0 \end{bmatrix} \begin{pmatrix} u \\ v \end{pmatrix} = \epsilon \begin{pmatrix} u \\ v \end{pmatrix}, \quad \tau(\mathbf{q}) = \sum_{i=1,2,3} t_i e^{i\mathbf{q} \cdot \mathbf{e}_i}, \quad (1)$$

where \mathbf{e}_i are vectors connecting a lattice site to its nearest neighbors, and u and v are wavefunction amplitudes on the two non-equivalent sublattices, A and B . The low-energy Hamiltonian for the valleys K and K' is obtained at $\mathbf{q} \approx \pm \mathbf{q}_0$, where $\pm \mathbf{q}_0$ are two non-equivalent Brillouin zone corners:

$$H_{\pm} = v \begin{bmatrix} 0 & ip_x \mp p_y + \frac{e}{c} a_{\pm} \\ -ip_x \mp p_y + \frac{e}{c} a_{\pm}^* & 0 \end{bmatrix} \quad (2)$$

with $a_{\pm} = \frac{e}{c} \sum_{i=1,2,3} \delta t_i e^{\pm i \mathbf{q}_0 \cdot \mathbf{e}_i}$, where the subscript $(+/-)$ corresponds to $K(K')$ valley. Decomposing $a_{\pm} = a_y \mp ia_x$, we see that the effective vector potential in the two valleys is given by $\pm(a_x, a_y)$. Notably, the field a is of opposite sign for the two valleys, thus preserving time-reversal symmetry (see Fig.1b).

Here we assume that the gauge field has white noise correlations with a correlation length ξ ,

$$\langle a_i(k)a_j(k) \rangle_{k\xi \ll 1} = \alpha^2, \quad a_i(k) = \int e^{-ikr} a_i(r) d^2r, \quad (3)$$

as appropriate for white noise fluctuations of δt_i . The fluctuating effective magnetic field can be estimated as

$$\delta h(x) = \partial_x a_y - \partial_y a_x \sim \alpha/\xi^2, \quad (4)$$

whereby the correlator of Fourier harmonics $\langle \delta h_k \delta h_{-k} \rangle$ behaves as k^2 at $k\xi \ll 1$.

Recently, strain-induced effective magnetic field was employed to explain anomalously small weak localization in graphene [14]. A direct observation of graphene ripples [14] yields typical corrugation length scale ξ of a few tens of nanometers. Estimates from the first principles [14] gave $\delta h \sim 0.1 - 1$ T, consistent with the observed degree of weak localization suppression.

Valley $K-K'$ asymmetry of QHFM in the presence of the gauge field (2) translates into a *uniaxial* random magnetic field, proportional to (4) and aligned with the pseudospin z axis. We shall see that the effect of random gauge field is subtle: somewhat counterintuitively, weak δh induces ordering in the system, acting as an easy plane anisotropy which favors the XY state. This behavior can be understood by noting that the transverse fluctuations in a ferromagnet are softer than the longitudinal fluctuations, making it beneficial for the spins to be polarized, on average, transversely to the field, as illustrated in Fig.2. This *random field-induced ordering* maximizes the energy gain of the spin system coupled to δh .

For magnets with uniaxial random field this behavior has been established [15, 16] in high space dimension. The situation in dimension two is considerably more delicate [17, 18] due to competition with the Larkin-Imry-Ma (LIM) [19, 20] disordered state. We shall see that the anisotropy induced by random gauge field is more robust than that due to random magnetic field. (This scenario is also relevant for the two-valley QH in AlAs system [21].)

The field-induced easy-plane anisotropy completely changes thermodynamics, transforming an O(3) ferromagnet, which does not order in 2d, to the XY model which exhibits a Berezinskii-Kosterlitz-Thouless transition to an ordered XY state. The transition temperature T_{BKT} is logarithmically renormalized by the out-of-plane fluctuations [22], $T_{BKT} \sim J/\ln(l_{XY}/\ell_B)$, where l_{XY} is the correlation length. For fields of the order of 30 T, with l_{XY} given by Eq.(15) below, we obtain T_{BKT} in the experimentally accessible range of a few Kelvin.

The XY-ordered QHFM state hosts fractional $\pm e/2$ charge excitations, so-called merons [7]. Merons are vortices such that in the vortex core the order parameter smoothly rotates out of the xy plane. There are four types of merons [7], since a meron can have positive or negative vorticity and the order parameter inside the core

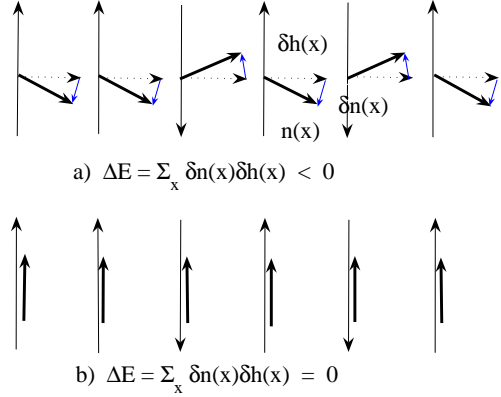


FIG. 2: Random field-induced order in a ferromagnet. The energy gained from the order parameter tilting opposite to the field is maximal when the spins and the field are perpendicular (a), and minimal for the spins parallel to the field (b). Uniaxial random field induces ordering in the transverse plane.

can tilt either in $+z$ or $-z$ direction. A pair of merons with the same charge and opposite vorticity is topologically equivalent to a skyrmion of charge $2(e/2) = e$ [7].

Turning to the discussion of QH effect, the hierarchy of the spin- and valley-polarized states is determined by relative strength of the Zeeman energy and the randomness-induced anisotropy. Our estimate below obtains the anisotropy of a few Kelvin at $B \sim 30$ T. This is smaller than the Zeeman energy in graphene, $\Delta_z = g\mu_B B \sim 50$ K at $B \sim 30$ T. Therefore we expect that $\nu = 0$ state is spin-polarized, with both valley states filled. (This was assumed in our previous analysis [23] of edge states in $\nu = 0$ state.) In contrast, in highly corrugated samples, when the anisotropy exceeds the Zeeman energy, an easy-plane valley-polarized $\nu = 0$ state can be favored.

While the character of $\nu = 0$ state is sensitive to the anisotropy strength, the $\nu = \pm 1$ states (see Fig.1a) are always both spin- and valley-polarized. Below we focus on $\nu = \pm 1$ states, keeping in mind that for strong randomnes our discussion also applies to $\nu = 0$ state.

Zeeman-split free Dirac fermion LL are given by

$$E_n = \text{sgn}(n)|2n|^{1/2} \frac{\hbar v}{\ell_B} \pm \Delta_z, \quad \ell_B = (\hbar c/eB)^{1/2}, \quad (5)$$

with n integer and $v \approx 8 \times 10^7$ cm/s. Each LL is doubly valley-degenerate. Random field (4) couples to electron orbital motion in the same way as the external field B , producing a local change in cyclotron energy and in the LL density. While the random field splits the $n \neq 0$ LL, for $n = 0$, it does not affect the single-particle energy (5) and couples to electron dynamics via exchange effects only. To estimate this coupling, we note that the field (4)

leads to valley imbalance in exchange energy per particle:

$$E_{K(K')} = E_{\text{exch}}(B \pm \delta h) = \frac{Ae^2}{\kappa\ell_B \pm \delta h}, \quad A = \left(\frac{\pi}{8}\right)^{1/2}, \quad (6)$$

where κ is the dielectric constant of graphene.

Let us analyze the graphene QHFM energy dependence on the gauge field. We consider a fully spin- and valley-polarized $\nu = -1$ state, described by a ferromagnetic order parameter $\mathbf{n} = (n_1, n_2, n_3)$ in the K, K' valley space. The valley-isotropic exchange interaction gives rise to a sigma model, with the gradient term only [6]:

$$E_0(n) = \frac{1}{2} \int J(\nabla \mathbf{n})^2 d^2x, \quad J = \frac{e^2}{64\kappa\ell_B}. \quad (7)$$

The valley-asymmetric coupling to δh in Eq.(6) generates a Zeeman-like Hamiltonian with a uniaxial random field.

$$E_1(n) = \int g\delta h(x)n_3(x)d^2x, \quad g = n \frac{dE_{\text{exch}}}{dB} = \frac{Ane^2}{2B\ell_B}, \quad (8)$$

where $n = 1/2\pi\ell_B^2$ is the electron density.

We estimate the energy gain from the order parameter $\mathbf{n}(x)$ correlations with the random field, treating the anisotropy (8) perturbatively in δh . Decomposing $\mathbf{n}(x) = \bar{\mathbf{n}} + \delta\mathbf{n}(x)$ and taking variation in $\delta\mathbf{n}$, we obtain

$$J\nabla^2\delta\mathbf{n} = g\delta\mathbf{h}_\perp, \quad \delta\mathbf{h}_\perp = (\mathbf{z} - \bar{\mathbf{n}}(\bar{\mathbf{n}} \cdot \mathbf{z}))\delta h.$$

Substituting the solution for $\delta\mathbf{n}$ into the energy functional (7), (8), we find an energy gain for $\bar{\mathbf{n}}$ of the form

$$\delta E = -\lambda \int (1 - \bar{n}_3^2(x))d^2x, \quad \lambda = \sum_k \frac{g^2 \langle \delta h_{-k} \delta h_k \rangle}{2Jk^2}, \quad (9)$$

where averaging over spatial fluctuations of δh is performed. This anisotropy favors the XY state, $\bar{n}_3 = 0$. Qualitatively (see Fig.2), the fluctuations due to $\delta\mathbf{n}$ tilting towards the z -axis minimize the energy of coupling to the uniaxial field when $\bar{\mathbf{n}}$ is transverse to it.

Now, let us compare the energies of the XY and the Larkin-Imry-Ma state [19, 20]. In LIM state the energy is lowered by domain formation such that the order parameter in each domain is aligned with the average field in this domain. Polarization varies smoothly between domains, and the typical domain size L is determined by the balance between domain wall and magnetic field energies. In our system, the LIM energy per unit area is

$$\varepsilon_{LIM} \sim -\frac{g\Phi(L)}{L^2} + \frac{J}{L^2}, \quad (10)$$

where $\Phi(L)$ is typical flux value through a region of size L . To estimate $\Phi(L)$ we write the magnetic flux through a region of size L as an integral of the vector potential over the boundary, which gives

$$\Phi(L) = \oint a_i(x) dx_i \sim \alpha\sqrt{L/\xi}. \quad (11)$$

Minimizing the LIM energy (10), we find

$$\varepsilon_{LIM} \sim -\frac{g^4\alpha^4}{J^3\xi^2}. \quad (12)$$

Comparison to the XY anisotropy $\lambda \sim -g^2\alpha^2/J\xi^2$ gives

$$\frac{\lambda}{\varepsilon_{LIM}} \sim \frac{J^2}{g^2\alpha^2} \sim \left(\frac{\Phi_0}{\Phi(\xi)}\right)^2, \quad \Phi_0 = hc/e, \quad (13)$$

where the flux through a region of size ξ where random field does not change sign. Interestingly, the ratio (13) does not depend on the external magnetic field. Therefore, at weak randomness, when the random field flux through an area ξ^2 is much smaller than the flux quantum, the ordered XY state has lower energy than the disordered LIM state.

In the opposite limit of strong randomness spins align with the local δh , forming a disordered state. It is instructive to note that for a model with white noise correlations of magnetic field, rather than of vector potential, the ratio (13) is of order one. In this case the competition of the LIM and the ordered states is more delicate.

A different perspective on the random-field-induced ordering is provided by analogy with the classical dynamics of a pendulum driven at suspension [24]. The latter, when driven at sufficiently high frequency, acquires a steady state with the pendulum pointing along the driving force axis. As discussed in Ref.[25], this phenomenon can be described by an effective potential U_{eff} obtained by averaging the kinetic energy over fast oscillations, with the minima of U_{eff} on the driving axis and maxima in the equatorial plane perpendicular to it. This behavior is robust upon replacement of periodic driving by noise [26]. Our statistical-mechanical problem differs from the pendulum problem merely in that the 1d time axis is replaced by 2d position space, which is inessential for the validity of the argument. The resulting effective potential is thus identical to that for the pendulum, with the only caveat related to the sign change $U_{\text{eff}} \rightarrow -U_{\text{eff}}$ in the effective action, as appropriate for transition from classical to statistical mechanics. Thus in our case the minima of U_{eff} are found in the equatorial plane, in agreement with the above discussion.

The easy-plane anisotropy (9) can be estimated as

$$\lambda/n \sim \frac{\delta h^2}{B^2} \times \frac{\xi^2}{\ell_B^2} \times \frac{e^2}{\kappa\ell_B} \approx 0.1 - 10 \text{ K/particle}, \quad (14)$$

where $\delta h \sim 0.1 - 1 \text{ T}$, $\xi \sim 30 \text{ nm}$ and $B \sim 30 \text{ T}$ was used. Since this is smaller than the Zeeman energy, we expect that the easy-plane ferromagnet in the valley space is realized at $\nu = \pm 1$, while $\nu = 0$ state is spin polarized with both valley states filled.

The out-of-plane fluctuations of the order parameter are characterized by the correlation length

$$l_{XY} \sim \sqrt{J/\lambda} \approx 1 - 10 \ell_B \quad (15)$$

for the above parameter values. The length l_{XY} sets a typical scale for order parameter change in the core of vortices (merons) as well as near edges of the sample and defects which induce non-zero z -component.

To measure the correlation length l_{XY} one may use the spatial structure of $\nu = 0$ wavefunction. Since the $K(K')$ electrons reside solely on either A or B sublattice, the order parameter z -component is equal to the density imbalance between the two sublattices. The latter can be directly measured by STM imaging technique.

Finally, we briefly outline the calculation of QHFM valley anisotropy for a pure graphene sheet (the details will be published elsewhere). Let us compare the energies of state 1, in which only the valley K (or K') Landau level is occupied, and state 2, with electrons in an equal-weight $K-K'$ superposition state. Since the $K(K')$ electrons at $\nu = 0$ reside on A (B) sublattice, the energies per particle in the Hartree-Fock approximation are given by

$$E_1 = \frac{n}{2} \sum_{\mathbf{r} \in A} v_0 V(r) \left(1 - e^{-r^2/2l_B^2}\right), \quad V(r) = \frac{e^2}{\kappa r},$$

$$E_2 = \frac{n}{4} \sum_{\mathbf{r} \in A,B} v_0 V(r) \left(1 - e^{-r^2/2l_B^2}\right),$$

where v_0 is unit cell volume. (Here we take $z = 0$ to be a site of the A sublattice.) We approximate the energy difference $E_1 - E_2$ by the Fourier harmonic of the Hartree-Fock energy density at the wave vector $|\mathbf{Q}| \sim 1/a$, where $a \approx 0.14$ nm is the graphene lattice spacing:

$$\Delta E = E_1 - E_2 \approx \frac{n}{4} \int V(r) \left(1 - e^{-r^2/2l_B^2}\right) e^{i\mathbf{Q}\mathbf{r}} d^2r.$$

With $Q\ell_B \sim \ell_B/a \gg 1$ at $B \simeq 30$ T, the integral yields

$$\Delta E \approx -\frac{27}{512\pi^3} \times \left(\frac{a}{\ell_B}\right)^3 \times \frac{e^2}{\kappa l_B} \simeq 10 \mu\text{K} \quad (16)$$

indicating that the anisotropy is negligible.

We note that the situation is completely different for higher LL. Goerbig et al. [9] pointed out that the Coulomb interaction can backscatter electrons of K and K' type at LL with $n \neq 0$, which leads to a much stronger lattice anisotropy of the order a/ℓ_B . This effect is absent for the zeroth LL due to the fact that K and K' states occupy different sublattices.

In summary, we studied the valley symmetry breaking of graphene QHFM. We considered the coupling of the strain-induced random magnetic field and found that it generates an easy-plane anisotropy, which is much stronger than the symmetry-breaking terms due to lattice. The estimates of the field-induced anisotropy suggest that the random field may be a principal mechanism of $K - K'$ QHFM symmetry breaking. The easy-plane ordered state is expected to exhibit BKT transition at experimentally accessible temperatures and half-integer charge excitations.

We are grateful to A. K. Geim, M. Kardar and P. Kim for useful discussions. This work is supported by NSF MRSEC Program (DMR 02132802), NSF-NIRT DMR-0304019 (DA, LL), and NSF grant DMR-0517222 (PAL).

-
- [1] K. S. Novoselov, A. K. Geim, S. V. Morozov, D. Jiang, Y. Zhang, S. V. Dubonos, I. V. Grigorieva, A. A. Firsov, *Science*, **306**, 666 (2004); *Proc. Natl. Acad. Sci. U.S.A.*, **102**, 10 451 (2005).
 - [2] K. S. Novoselov, A. K. Geim, S. V. Morozov, D. Jiang, M. I. Katsnelson, I. V. Grigorieva, S. V. Dubonos, A. A. Firsov, *Nature* **438**, 197 (2005).
 - [3] Y. Zhang, Y.-W. Tan, H. L. Stormer and P. Kim, *Nature* **438**, 201 (2005).
 - [4] Y. Zhang, Z. Jiang, J. P. Small, M. S. Purewal, Y. W. Tan, M. Fazlollahi, J. D. Chudow, J. A. Jaszczak, H. L. Stormer, and P. Kim, *Phys. Rev. Lett.*, **96**, 136806 (2006).
 - [5] For a review, see article by S. M. Girvin and A. H. MacDonald in *Perspectives in Quantum Hall Effects*, S. Das Sarma and A. Pinczuk, Eds. (Wiley, New York, 1997).
 - [6] K. Yang, K. Moon, L. Zheng, A. H. MacDonald, S. M. Girvin, D. Yoshioka, and S.-C. Zhang, *Phys. Rev. Lett.* **72**, 732 (1994).
 - [7] K. Moon, H. Mori, K. Yang, S. M. Girvin, A. H. MacDonald, L. Zheng, D. Yoshioka, and S.-C. Zhang, *Phys. Rev. B* **51**, 5138 (1995).
 - [8] K. Nomura and A. H. MacDonald, *Phys. Rev. Lett.* **96**, 256602 (2006)
 - [9] M. O. Goerbig, R. Moessner and B. Douçot, cond-mat/0604554, unpublished.
 - [10] J. Alicea and M. P. A. Fisher, *Phys. Rev. B* **74**, 075422 (2006)
 - [11] S. V. Iordanskii and A. E. Koshelev, *ZETF Pisma*, **41**, 471 (1985) [translation: *JETP Lett.* **41**, 574 (1985)].
 - [12] C. L. Kane and E. J. Mele, *Phys. Rev. Lett.* **78**, 1932 (1997).
 - [13] A. Morpurgo and F. Guinea, cond-mat/0603789.
 - [14] S. V. Morozov, K. S. Novoselov, M. I. Katsnelson, F. Schedin, L. A. Ponomarenko, D. Jiang, and A. K. Geim, *Phys. Rev. Lett.* **97**, 016801 (2006).
 - [15] A. Aharony, *Phys. Rev. B* **18**, 3328 (1978).
 - [16] D. E. Feldman, *J. Phys. A: Math. Gen.* **31**, 177 (1998).
 - [17] B. J. Minchau and R. A. Pelcovits, *Phys. Rev. B* **32**, 3081 (1985).
 - [18] J. Wehr, A. Niederberger, L. Sanchez-Palencia and M. Lewenstein, cond-mat/0604063.
 - [19] A. I. Larkin, *JETP* **31**, 784 (1970).
 - [20] Y. Imry and S. K. Ma, *Phys. Rev. Lett.* **35**, 1399 (1975).
 - [21] Y. P. Shkolnikov, S. Misra, N. C. Bishop, E. P. De Poortere, and M. Shayegan, *Phys. Rev. Lett.* **95**, 066809 (2005)
 - [22] S. Hikami, T. Tsuneto, *Progr. Theor. Phys.* **63**, 387 (1980).
 - [23] D. A. Abanin, P. A. Lee and L. S. Levitov, *Phys. Rev. Lett.* **96**, 176803 (2006).
 - [24] P. L. Kapitza, *Zh. Eksp. Teor. Fiz.*, **21**, 588 (1951).
 - [25] L. D. Landau and E. M. Lifshitz, Mechanics, Chap. V, §30, (Reed Educational and Professional Publ. Ltd, 2002)
 - [26] R. L. Stratovich and Yu. M. Romanovsky, *Nauch. Dokl. Vys. Shk., ser. fiz.-mat.* **3**, 221 (1958) (in Russian).